Reversal mechanisms in perpendicularly magnetized nanostructures

Justin M. Shaw and Stephen E. Russek
National Institute of Standards and Technology, Boulder, Colorado 80305, USA

Thomas Thomson
School of Computer Science at the University of Manchester, Manchester M13 9PL, United Kingdom and Hitachi Global Storage Technology, San Jose, California 95135, USA

Michael J. Donahue
National Institute of Standards and Technology, Gaithersburg, Maryland 20899, USA

Bruce D. Terris, Olav Hellwig, and Elizabeth Dobisz
Hitachi Global Storage Technology, San Jose, California 95135, USA

Michael L. Schneider
Department of Physics and Astronomy at the University of Montana, Missoula, Montana 59812, USA
(Received 28 April 2008; published 16 July 2008)

We demonstrate that magnetic reversal in perpendicularly magnetized nanostructures is highly dependent on the nature and condition of the edges. To understand the impact of edge damage, we compare nanostructures created by ion milling to those prepared on prepatterned substrates. The size- and temperature-dependent reversal properties of 25 nm–1 μm diameter nanodots show that reversal in prepatterned nanostructures is controlled by nucleation within the interior, whereas ion milling results in an edge nucleation process with an unpredicted temperature dependence of the reversal field.

DOI: 10.1103/PhysRevB.78.024414 PACS number(s): 75.60.Jk, 75.75.+a

I. INTRODUCTION

Magnetic nanostructures have potential applications in emerging technologies including spintronics,[1,2] bit patterned media,[3–6] magnetic random access memory,[7] and magnetic-field sensors. Many of these technologies now incorporate materials with perpendicular magnetic anisotropy. While significant work has been done on reversal modes for in-plane magnetic nanostructures,[8] the reversal mode of high anisotropy, perpendicularly magnetized nanostructures has been less well studied. In particular, the nanoscale variations induced by different fabrication methods have not been reported.

When a magnetic structure reaches dimensions below a critical size, single domain behavior is generally approximated by the Stoner-Wohlfarth (S-W) mode, whereby the magnetic moments undergo coherent rotation in response to an applied magnetic field. The time and temperature-dependent switching field (H_{sf}) is then described by the Sharrock formalism.[9] According to our results, however, this formalism does not accurately predict the temperature dependence of H_{sf} for certain nanoscale switching modes.

An important property of an ensemble of magnetic nanostructures is its switching field distribution (SFD), whereby nominally identical structures have different values of H_{sf}. Broad and uncontrollable SFDs impede the development of technologies that rely on uniform arrays of magnetic nanostructures. Currently, the origin of SFDs is not fully understood and is a source of debate.[3–5,10–14] A fundamental understanding of the reversal mechanism is the critical first step in both isolating the underlying physical causes of SFDs and providing methods of controlling switching fields in ensembles of magnetic nanostructures. As an example, it has been recently shown that an intrinsic distribution of local magnetic anisotropy energies applied to the Sharrock formalism explains SFDs in certain Co/Pd nanostructures.[3] In that case, modeling the switching as a modified S-W reversal mode restricted to a nucleation volume provided good agreement with the experiment.

In this paper, we demonstrate, via the diameter and temperature dependence of H_{sf} in nanodot arrays, that two different reversal mechanisms can result from only a small change in the edge properties. We present numerical simulations that show how the reversal process changes when edge modification is present and demonstrate qualitative agreement with experimental data.

II. EXPERIMENT

Two fabrication processes were used in this study: (1) deposition of a continuous magnetic thin film followed by ion milling; and (2) deposition of a magnetic thin film onto a prepatterned Si substrate. In both cases, the magnetic layer is a sputter-deposited Co/Pd multilayer consisting of eight bilayers with a Co layer thickness ranging from 0.28 to 0.33 nm and a Pd thickness ranging from 0.89 to 0.96 nm. The Co/Pd multilayers were deposited on either a thicker Pd or a Ta seed layer.[4] The magnetic properties of the thin films were characterized using a superconducting quantum interference device (SQUID) magnetometer.

Patterning in both processes consists of an electron-beam lithography lift-off process to create a Cr etch mask. The mask is transferred to the continuous thin film in process 1

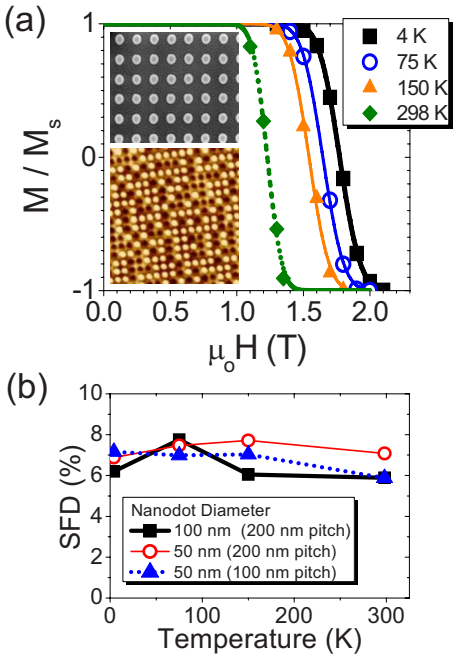

FIG. 1. (Color online) (a) Remanent hysteresis curves with integrated Gaussian distribution fits at various temperatures for an ion milled 50 nm diameter sample and corresponding SEM (top inset) and MFM (bottom inset) images. (b) The temperature dependence of the SFDs.

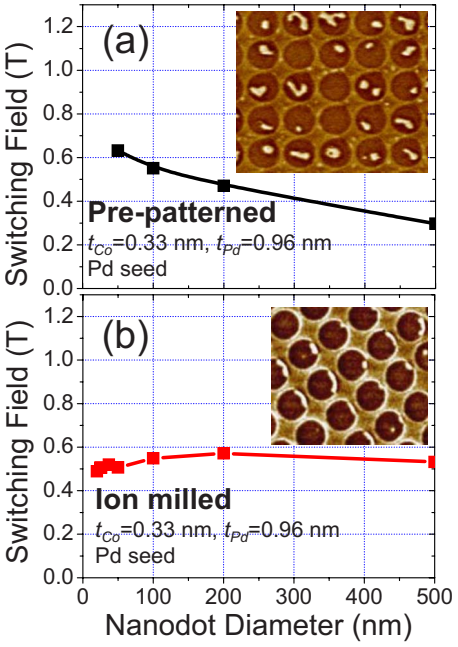

FIG. 2. (Color online) The diameter dependence of H_{sf} for the (a) prepatterned and (b) ion milled samples. The insets in (a) and (b) show the corresponding MFM images of the nucleation sites in $d=1$ μm dots induced with an in-plane field.

via a 300 eV Ar ion mill, whereas in process 2, a reactive ion etch is used to transfer the pattern to the Si substrate. Samples fabricated by process 1 and process 2 will be referred to as "ion milled" and "prepatterned," respectively. The details of both of these processes are given in Refs. 4 and 15. A scanning electron microscope (SEM) image and a magnetic force microscope (MFM) image of a resulting array of 50 nm nanostructures can be seen in the insets of Fig. 1(a).

The remanent magnetization state of the samples, and hence H_{sf}, was measured either by remanent magneto-optic Kerr-effect hysteresis curves or by a series of MFM images. The latter method was used to obtain the temperature T dependence. In this method, the sample is first cooled to a given temperature and then saturated prior to the application of a reverse magnetic field. The magnetic field is subsequently removed and the sample brought to room temperature for MFM imaging. The remanence curve is produced by repeating this process for several applied field values and counting the number of nanodots that reversed. An integrated Gaussian distribution (error function) is fitted to the data in order to obtain H_{sf} (mean) and the SFD (standard deviation).

Figure 1(a) shows a series of remanent hysteresis curves as a function of T for an ion milled 50 nm sample. The *relative* SFD (taken as SFD/H_{sf}) is constant with temperature, as shown in Fig. 1(b) for three different ion milled arrays, indicating that SFDs are not caused by random thermal fluctuations. The relatively flat temperature dependence of the SFDs also suggests that the switching fields maintain the same relative temperature dependence for the highest and lowest anisotropy structures, which is important when comparing and fitting the temperature dependence of H_{sf}.

Micromagnetic simulations were performed using object oriented micromagnetic framework (OOMMF) (Ref. 16) with either a cubic cell with size of 1 nm^3 or a square prism with size of $1\times1\times3$ nm^3. No significant difference was observed using either cell configuration. The magnetic parameters used in the simulations were as follows: volume magnetization $M_s=5\times10^5$ A/m, anisotropy energy density $K=8\times10^5$ J/m^3, the Gilbert damping constant $\alpha=0.1$,[17] and the exchange stiffness constant $A=1\times10^{-11}$ J/m, which was estimated from measurements of the low-temperature dependence of M_s. These values are median values measured in Co/Pd samples used in this study. However, the magnetic properties of Co/Pd can vary dramatically depending on deposition conditions, seed layers, and thickness of layers.[4] All simulations were done without a random thermal field (therefore corresponding to $T\approx0$ K) and with a small in-plane field equivalent to a $3°-4°$ field misalignment to break the symmetry.

III. RESULTS AND DISCUSSION

A. Size-dependent reversal properties

The diameter dependence of H_{sf} for the prepatterned and ion milled samples is given in Figs. 2(a) and 2(b), respectively. Two trends are observed in the plots. The prepatterned data show a gradual increase in switching field as d is reduced, as expected.[3] However, the ion milled sample shows a maximum in H_{sf} at approximately 200 nm. This suggests that the ion milling process alters the magnetic properties of the edges, since such effects would have a larger influence as d is reduced.

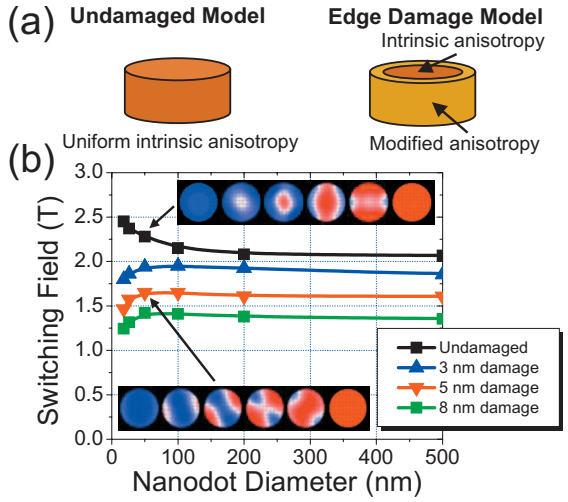

FIG. 3. (Color) (a) Schematic of the model used to include edge damage in the OOMMF simulations; (b) the diameter dependence of the switching field from OOMMF simulation results for various values of edge damage. The insets in (b) show the time evolution in a 50 nm nanodot as it undergoes reversal in the undamaged (top) and edge damaged (bottom) cases over a time of approximately 1 ns. The color scale represents the z component of the magnetization.

In order to explain the data in Figs. 2(a) and 2(b), micromagnetic simulations were performed with and without edge anisotropy modification. Figure 3(a) shows a schematic of how edge anisotropy modification was modeled in the micromagnetic simulations. We assumed a 50% reduced anisotropy, confined to only a few nanometers at the edge (hereafter referred to as "edge damage"). We believe a 50% reduction in anisotropy is a reasonable value, since the anisotropy has been shown to profoundly decrease and even undergo a sign change (i.e., becoming an in-plane one) with a small ion radiation dose.[18–20]

In the case of uniform anisotropy, reversal is nucleated in a volume located at the center or interior of the nanodot—since the edges are stiffer due to the additional energy arising from the generation of magnetostatic edge charges—as shown in the upper inset of Fig. 3(b). However, with only a few nanometers of edge damage, the nanodot exhibits edge nucleated reversal, which leads to a significantly lower switching fields as shown in Fig. 3(b). In addition, the simulations show that H_{sf} increases as the nanodot diameter is reduced in the case of uniform anisotropy, which can be explained solely from the change in shape anisotropy as d decreases. However, when edge damage is present, H_{sf} reaches a maximum and then decreases as d decreases.

The fact that the simulated data for various values of edge damage do not converge at larger diameters indicates that a reduction in average anisotropy is not enough to explain the reduction in H_{sf}. In other words, the energy barrier for reversal is reduced for a nucleation volume at the lower anisotropy edge region and is largely independent of the size of the higher anisotropy interior region when d is above 200 nm.

Micromagnetic simulations also show that as the diameter d decreases below 25 nm, the entire nanodot undergoes a single coherent rotation reversal mode, independent of the presence of edge damage. This is expected as the nanodot dimensions approach the exchange length.

The micromagnetic simulation results, along with the data in Figs. 2(a) and 2(b), are consistent with the ion milling process significantly altering the anisotropy at the edges, resulting in edge nucleated reversal. In contrast, samples prepared via deposition on a prepatterned wafer have a more uniform anisotropy with a center nucleated reversal process. The shift in H_{sf} between the two samples in Figs. 2(a) and 2(b) results from the fact that the Co/Pd multilayer films had different values of M_s and anisotropy K. The additional negative slope present in the data for the prepatterned sample is the result of an intrinsic distribution of local anisotropies.[3] This random distribution of local anisotropies is not included in the present model; therefore, its effect on nanostructures with edge damage is not known.

B. Imaging of nucleation sites

Nucleation sites can be experimentally identified in larger diameter structures by applying an in-plane magnetic field and imaging the remanent state with MFM.[21] In this case, d must be high enough for the structure to exist in a stable multidomain state. The insets of Figs. 2(a) and 2(b) show the imaged nucleation sites in arrays of 1 μm structures. In the case of the prepatterned wafer, almost all the nucleation sites are in the interior region. In contrast, the ion milled sample has a majority of nucleation sites located at the edge. These images clearly support the idea that ion milling lowers the anisotropy at the edges. Note that edge nucleation sites were also previously observed in granular CoCrPt nanodot arrays prepared by focused ion beam, where the ion induced damage would likely be more severe.[22]

C. Temperature-dependent reversal properties

Further insight into the effects of edge damage on the reversal mechanism can be gained by examining the temperature dependence of H_{sf}. In order to model the temperature-dependent reversal properties of the nanodots, the intrinsic properties of the thin films were first determined. Thin film samples, taken from the same wafer used to fabricate the nanostructures, were measured using a SQUID magnetometer to determine the temperature dependence of the effective anisotropy field $H_k^{\text{eff}}(T)$ and $M_s(T)$. $H_k^{\text{eff}}(T)$ was determined from the saturation point of the in-plane hysteresis curves and was roughly linear with respect to T. $H_k^{\text{eff}}(T)$ was therefore fitted to a line for analytical modeling. The intrinsic anisotropy energy density $K^{\text{film}}(T)$ is determined from the effective anisotropy field by the following relation: $H_k^{\text{eff}}(T)=[2K^{\text{film}}(T)/\mu_0 M_s(T)]-M_s(T)$, where μ_0 is the permeability constant. The temperature dependence of M_s was fitted to $M_s(T)=M_s^{0\ \text{K}}[1-(T/\Theta)^{3/2}]$, where the two fitting parameters $M_s^{0\ \text{K}}$ and Θ are the magnetization at 0 K and a characteristic temperature, respectively. Examples of the temperature dependence of both H_k^{eff} and M_s and corresponding fits are shown in Figs. 4(a) and 4(b), respectively.

The anisotropy energy density of a nanodot is then approximated by

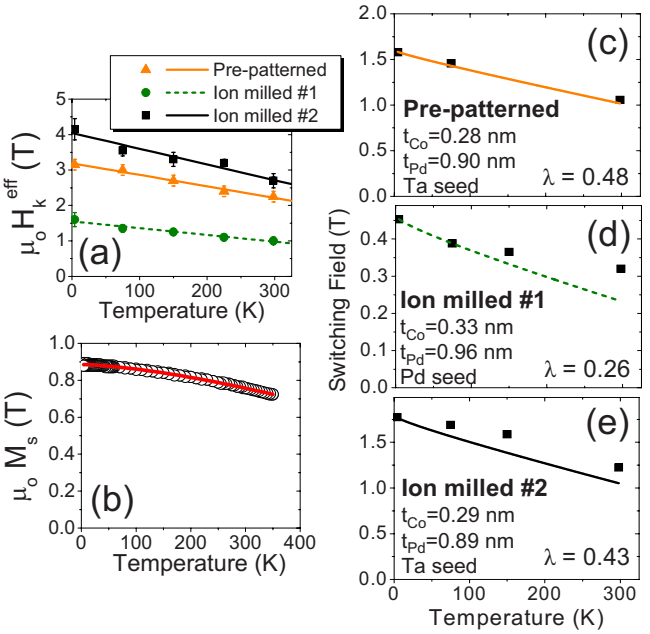

FIG. 4. (Color online) The temperature dependence of (a) H_k^{eff} and (b) M_s for some continuous Co/Pd multilayers, and the switching field for the (c) prepatterned and [(d) and (e)] ion milled samples. Fits using Eq. (2) are included in (c)–(e) as well as values of the correction factor λ used in the fits.

$$K^{\text{dot}}(T) = \left[\frac{\mu_0 M_s(T)}{2}\right][H_k^{\text{eff}}(T) + (1 - N_{zz} + N_{xx})M_s(T)]. \tag{1}$$

Here, N_{zz} and N_{xx} are the perpendicular and in-plane demagnetization factors, respectively. For the analytic modeling described here, these were calculated using formulas for equivalent rectangular prisms.[23]

Figures 4(c)–4(e) show the temperature-dependent switching field data for 100 nm diameter prepatterned and two ion milled nanostructures, respectively. If the nucleation volume reverses according to the S-W mode, the time and temperature dependence of H_{sf} will be described by the Sharrock formalism, Eq. (2) (Ref. 9):

$$H_{\text{sf}}(T,\tau) = \left[\frac{2K^{\text{dot}}(T)}{\mu_0 M_s(T)}\right]\left[1 - \sqrt{\frac{k_B T}{K^{\text{dot}}(T)V}\ln\left(\frac{f_0\tau}{\ln 2}\right)}\right]\lambda. \tag{2}$$

Here, V is the nucleation volume, k_B is Boltzmann's constant, $\tau = 10$ s is the applied field time, and $f_0 = 10$ GHz is the attempt frequency. λ is a correction factor since H_{sf} is generally lower than the theoretical value.[9] V was estimated using a nucleation length of 20 nm and the thickness of the film (a nucleation length of 20 nm corresponds to the upper limit of the exchange length and is consistent with the nucleation volume observed in micromagnetic simulations).

The comparison of Figs. 4(c)–4(e) shows that the temperature-dependent switching field data for the prepatterned sample agree with Eq. (2) reasonably well, but the data from the ion milled samples do not. The data for the ion milled sample show a temperature dependence of H_{sf} that is less than that predicted by Eq. (2). In these plots, the only adjustable parameter was λ, which was optimized to bring the values of H_{sf} into agreement at 4 K. Fits of the ion milled data were also performed by allowing V, $M_s(T)$, and $K^{\text{dot}}(T)$ to vary, but no significant improvements were achieved—unless those parameters reached unphysical values.

The reduced temperature dependence of H_{sf} for the ion milled data suggests that the reversal mechanism is altered with the presence of edge damage. It also indicates that the reversal process cannot be simply described by a change in the location of the nucleation volume from the interior region to the edge region. The discrepancy between the ion milled data and Eq. (2) can originate from several possible sources:

(1) The energy barrier for reversal may not be that of the ideal S-W mode, since the boundary conditions (both in terms of exchange and magnetostatic components) for a nucleation volume at the interior versus the edge can be different. In particular, reversal may occur via multiple energy barriers as previously observed in nanowires.[24]

(2) The temperature dependence of the magnetic properties may be significantly altered at the edge, which cannot be approximated by a trivial modification of the undamaged magnetic properties. The need for a nontrivial modification of magnetic properties is supported by the fact that fits of the ion milled data to Eq. (2) did not improve significantly when the fitting parameters for $M_s(T)$ and $K^{\text{dot}}(T)$ were allowed to vary. Thus, the functional form of $M_s(T)$ or $K^{\text{dot}}(T)$ would have to be altered, which is unlikely.

(3) The reversal mechanism itself may be a function of temperature, depending on the relative temperature-dependent properties of edge versus center material. In other words, for one temperature range, the edge properties may dominate the reversal, but the interior material may dominate reversal in a different temperature range. However, the fact that the SFD [Fig. 1(b)] is constant in temperature strongly argues against this assumption, since in that case, the SFD would likely differ for nucleation occurring at the damaged edge region versus the interior region.

(4) Micromagnetic simulations indicate that reversal occurs in the nanodots via a nucleation and propagation event for diameters greater than 25 nm. As a result, the reversal process may be a competition between the nucleation field and the pinning field. Both of these fields would be expected to vary significantly in magnitude for ion milled (edge nucleation) and prepatterned (interior nucleation) samples. Most importantly though, the temperature dependence of the pinning field would not likely follow Eq. (2), which describes the nucleation volume. This picture is further supported by the results of Wernsdorfer *et al.*,[25] which demonstrate that pinning fields in certain Ni nanowires have a significantly reduced temperature dependence relative to that of the nucleation fields.

Although the study presented here focuses on Co/Pd multilayers, our results can be applied to most materials with perpendicular anisotropy including many perpendicular spintronic structures currently under development, such as Ni/Co.[1,2] In particular, multilayer systems are extremely sensitive to ion damage since the anisotropy is highly dependent on the interface and/or microstructure. However, these ef-

fects are not strictly confined to multilayers as observed in ion irradiation studies of granular CoCrPt.[22] We note that the expression "edge damage" is used to describe any reduction in edge anisotropy resulting from either shape or intrinsic means. This damage can originate from a number of sources, including ion induced intermixing of interfaces, ion induced damage of the microstructure, redeposition of magnetic material during etching, oxidation of edges, edge roughness, side tapering, and material segregation at the edge. In order to fully realize the effect of edge damage on SFDs, the edge damage model must be incorporated along with a random distribution of intrinsic anisotropies.

IV. CONCLUSIONS

We have shown through the diameter and temperature dependence of H_{sf}, micromagnetic simulations, and MFM imaging of nucleation sites that the edge properties of perpendicularly magnetized nanostructures can alter the reversal mechanism. If the nanostructure is approximately homogeneous throughout its entire volume, the system prefers a center nucleation reversal process that is well described by the Sharrock formalism. In contrast, a small amount of edge damage from ion milling results in an edge nucleation process. Consequently, care must be taken when artificially structured magnetic materials are studied, compared, or modeled since the preparation process will strongly influence the magnetic and reversal properties.

ACKNOWLEDGMENTS

The authors are grateful to Tom Silva, Hans Nembach, and Alina Deac for valuable discussions; Donna Hurley for use of her MFM system; and Miles Olsen for programing help.

[1] S. Mangin, D. Ravelosona, J. A. Katine, M. J. Carey, B. D. Terris, and E. E. Fullerton, Nature (London) **5**, 210 (2006).
[2] D. Houssameddine, U. Ebels, B. Delaët, B. Rodmacq, I. Firastrau, F. Ponthenier, M. Brunet, C. Thirion, J.-P. Michel, L. Prejbeanu-Buda, M.-C. Cyrille, O. Redon, and B. Dieny, Nat. Mater. **6**, 447 (2007).
[3] T. Thomson, G. Hu, and B. D. Terris, Phys. Rev. Lett. **96**, 257204 (2006).
[4] J. M. Shaw, W. H. Rippard, S. E. Russek, T. Reith, and C. M. Falco, J. Appl. Phys. **101**, 023909 (2007).
[5] O. Hellwig, A. Berger, T. Thomson, E. Dobisz, Z. Z. Bandic, H. Yang, D. S. Kercher, and E. E. Fullerton, Appl. Phys. Lett. **90**, 162516 (2007).
[6] C. E, D. Smith, J. Wolfe, D. Weller, S. Khizroev, and D. Litvinov, J. Appl. Phys. **98**, 024505 (2005).
[7] S. Assefa, J. Nowak, J. Z. Sun, E. O'Sullivan, S. Kanakasabapathy, W. J. Gallagher, Y. Nagamine, K. Tsunekawa, D. D. Djayaprawira, and N. Watanabe, J. Appl. Phys. **102**, 063901 (2007).
[8] Y. Acremann, J. P. Strachan, V. Chembrolu, S. D. Andrews, T. Tyliszczak, J. A. Katine, M. J. Carey, B. M. Clemens, H. C. Siegmann, and J. Stöhr, Phys. Rev. Lett. **96**, 217202 (2006).
[9] M. P. Sharrock and J. T. McKinney, IEEE Trans. Magn. **17**, 3020 (1981).
[10] M. L. Schneider, M. R. Pufall, W. H. Rippard, S. E. Russek, and J. A. Katine, Appl. Phys. Lett. **90**, 092504 (2007).
[11] Y. Kitade, H. Komoriya, and T. Maruyama, IEEE Trans. Magn. **40**, 2516 (2004).
[12] C. Haginoya, S. Heike, M. Itabashi, K. Nakamura, and K. Koike, J. Appl. Phys. **85**, 8327 (1999).
[13] J. W. Lau, R. D. McMichael, S. H. Chung, J. O. Rantschler, V. Parekh, and D. Litvinov, Appl. Phys. Lett. **92**, 012506 (2008).
[14] M. J. Donahue, G. Vertesy, and M. Pardavi-Horvath, J. Appl. Phys. **93**, 7038 (2003).
[15] G. Hu, T. Thomson, M. Albrecht, M. E. Best, B. D. Terris, C. T. Rettner, S. Raoux, G. M. McClelland, and M. W. Hart, J. Appl. Phys. **95**, 7013 (2004).
[16] M. J. Donahue and D. G. Porter, National Institute of Standards and Technology Interagency, Report No. 6376, (NIST, Gaithersburg, 1999), http://math.nist.gov/oommf
[17] A. Barman, S. Wang, O. Hellwig, A. Berger, E. E. Fullerton, and H. Schmidt, J. Appl. Phys. **101**, 09D102 (2007).
[18] V. Parekh, D. Smith, C. E. J. Rantscher, S. Khizroev, and D. Litvinov, J. Appl. Phys. **101**, 083904 (2007).
[19] R. Hyndman, P. Warin, J. Gierak, J. Ferre, J. N. Chapman, J. P. Jamet, V. Mathet, and C. Chappert, J. Appl. Phys. **90**, 3843 (2001).
[20] C. T. Rettner, S. Anders, J. E. E. Baglin, T. Thomson, and B. D. Terris, Appl. Phys. Lett. **80**, 279 (2002).
[21] G. Hu, T. Thomson, C. T. Rettner, and B. D. Terris, IEEE Trans. Magn. **41**, 3589 (2005).
[22] C. T. Rettner, S. Anders, T. Thomson, M. Albrecht, Y. Ikeda, M. E. Best, and B. D. Terris, IEEE Trans. Magn. **38**, 1725 (2002).
[23] A. Aharoni, J. Appl. Phys. **83**, 3432 (1998).
[24] W. Wernsdorfer, B. Doudin, D. Mailly, K. Hasselbach, A. Benoit, J. Meier, J.-Ph. Ansermet, and B. Barbara, Phys. Rev. Lett. **77**, 1873 (1996).
[25] W. Wernsdorfer, K. Hasselbach, A. Benoit, B. Barbara, B. Doudin, J. Meier, J.-Ph. Ansermet, and D. Mailly, Phys. Rev. B **55**, 11552 (1997).